Alexandria Engineering Journal (2016) 55, 2139–2148

HOSTED BY

ELSEVIER

Alexandria University

Alexandria Engineering Journal

www.elsevier.com/locate/aej
www.sciencedirect.com

ORIGINAL ARTICLE

Hydromagnetic Falkner-Skan flow of Casson fluid past a moving wedge with heat transfer

Imran Ullah [a], **Ilyas Khan** [b], **Sharidan Shafie** [a,*]

[a] *Department of Mathematical Sciences, Faculty of Science, Universiti Technologi Malaysia, 81310 UTM Johor Bahru, Johor, Malaysia*
[b] *Basic Sciences Department, College of Engineering Majmaah University, P.O. Box 66, Majmaah 11952, Saudi Arabia*

Received 27 February 2016; revised 15 June 2016; accepted 25 June 2016
Available online 19 July 2016

KEYWORDS

Casson fluid;
Moving wedge;
Viscous dissipation;
Heat generation/absorption

Abstract Numerical solutions are carried out for steady state two dimensional electrically conducting mixed convection flow of Casson fluid along non-isothermal moving wedge through porous medium in the presence of viscous dissipation and heat generation/absorption. The governing partial differential equations, subject to boundary conditions are transformed into ordinary differential equations using similarity transformations. The transformed equations are then solved numerically by Keller-box method. To check the validity of present method, numerical results for dimensionless local skin friction coefficient and rate of heat transfer are compared with results of available literature as special cases and revealed in good agreement. The influence of pertinent parameters on velocity, temperature profiles, as well as wall shear stress and heat transfer rate is displayed in graphical form and discussed. It is found that fluid velocity increases with increase of Eckert number in case of assisting flow, while it decreases in case of opposing flow. It is also noticed that heat generation/absorption parameter influence fluid velocity and temperature significantly. A significant result obtained from this study is that heat transfer rate reduces with increase of Prandtl number in the presence of viscous dissipation effect. Also, increasing values of Eckert number have no effects on force convection flow.

1. Introduction

The study of the flow field in a boundary adjacent to the wedge is very important, and is an essential part in the area of fluid dynamics and heat transfer. Especially, convectional flow of Newtonian and non-Newtonian fluid over the wedge becomes important currently. The pioneer work of Falkner-Skan [1] has been extended by Rajagopal et al. [2] to second grade fluid over wedge placed static inside the fluid. Later, Lin and Lin [3] explored the characteristics of heat transfer in force convection flow past a static wedge for any Prandtl number. Watanabe [4] and Pop and Watanabe [5] investigated force and free convection boundary layer flow past a wedge, respectively. Motivated by this, Kumari et al. [6] theoretically investigated mixed convection flow over a wedge saturated in a porous medium under the influence of magnetic field. Chamkha et al. [7] examined the effects of thermal radiation on force convection along non-isothermal wedge.

* Corresponding author.

Peer review under responsibility of Faculty of Engineering, Alexandria University.

http://dx.doi.org/10.1016/j.aej.2016.06.023

Further, Ishak et al. [8,9] analyzed boundary layer flow over a wedge moving in micropolar and viscous fluid, respectively. The influence of suction or injection on mixed convection flow of second grade viscoelastic fluid over permeable wedge is reported by Hsiao [10]. An analytical solution of mixed convection flow over porous wedge in the presence of thermal radiation is found by Su et al. [11]. The effect of suction/blowing on force convection flow of Casson fluid caused by wedge placed symmetrical to the fluid is presented by Mukhopadhyay et al. [12]. The characteristics of heat transfer on mixed convection flow of viscoelastic fluid along a permeable wedge under the influence of magnetic field is reported by Rashidi et al. [13]. Recently, El-Dabe et al. [14] obtained numerical solutions for electrically conducting forced convection flow of Casson fluid over a moving wedge.

In addition to convection heat transfer flow, the effect of viscous dissipation and heat generation or absorption cannot be ignored, as it has direct impact on heat transfer. For this reason, both become essential in many physical situations, viz. rocket engine, electronic chips, thermal insulation, semiconductor wafers and cooling of nuclear reactor. Keeping in view of its applications, Gebhart [15] for the first time included the effects of viscous dissipation in free convection. Later on, Yih [16] explored the effects of viscous dissipation on force convection flow caused by non-isothermal wedge under the influence of magnetic field. The numerical results are obtained by employing Keller-box method. Kandasamy et al. [17] analyzed mixed convection flow of viscous fluid past a wedge in the presence of viscous dissipation numerically. The steady state, two dimensional boundary layer flow adjacent to the wedge in the presence of viscous dissipation and heat generation or absorption is discussed by Pal and Mondal [18]. They obtained the non-similar solution by using Runge-Kutta-Fehlberg scheme. They noticed that fluid temperature falls as Eckert number increases. The influence of heat generation or absorption on mixed convection flow caused by stationary wedge is provided by Ganapathirao et al. [19]. Numerical investigations on mixed convection flow of viscous fluid over a porous non-isothermal wedge in the presence of viscous dissipation and heat generation or absorption are carried out by Prasad et al. [20]. They concluded that Eckert number and heat source/sink parameter enhance the temperature significantly.

Ahmad and Khan [21] examined the influence of viscous dissipation and heat generation or absorption on force convection flow of viscous fluid over a moving wedge subject to suction/injection. They observed that temperature is higher in the presence of heat source. Khan et al. [22] obtained numerical results of electrically conducting flow caused by moving wedge in the presence of heat generation or absorption. They solved the governing equations with the help of shooting method together with Runge-Kutta-sixth order scheme. The effects of heat generation or absorption and chemical reaction on mixed convection flow along a vertical wedge subject to suction or injection are discussed by Ganapathirao et al. [23]. Very recently, Kasmani et al. [24] explored the effects of heat generation on force convection flow over a wedge placed static in the nanofluid numerically. They concluded that increasing values of heat generation or absorption parameter leads to higher temperature.

The above discussion and applications in existing literature are the source of motivation to investigate the effects of viscous dissipation and heat generation or absorption on mixed convection flow of Casson fluid over a moving wedge under the influence of magnetic field. The non-linear partial differential equations transformed into non-linear ordinary differential equations with the help of similarity transformation. The highly nonlinear transformed equations are solved numerically by using an implicit finite difference scheme known as Keller-box method [25]. Comparisons of some special cases are made with the results of available literature and found in good agreement.

2. Mathematical formulation

A steady mixed convection flow of Casson fluid over a moving wedge through porous medium in the presence of magnetic field is considered. It is assumed that wedge is moving with the velocity $u_w(x) = U_w x^m$ and the free stream velocity $u_e(x) = U_\infty x^m$, where U_w and U_∞ are constants. Here $\lambda = \frac{2m}{m+1}$ is the Hartree pressure gradient parameter corresponding to $\lambda = \frac{\Omega}{\pi}$ for the total angle Ω of the wedge (see Fig. 1). It is also assumed that the induced magnetic field caused by the motion of electrically conducting fluid is neglected, as it is very small compared to magnetic field. Further, the buoyancy force generates due to temperature differences inside moving fluid, and is taken in momentum equation. The effects of viscous dissipation and heat generation/absorption are included in present study. Further, the wall of wedge is heated by variable temperature $T_w(x) = T_\infty + Ax^{2m}$ and free stream temperature is denoted by T_∞.

The rheological governing equations for momentum and energy are given as

$$\frac{\partial u}{\partial x} + \frac{\partial v}{\partial x} = 0, \tag{1}$$

$$u\frac{\partial u}{\partial x} + v\frac{\partial u}{\partial y} = u_e\frac{\partial u_e}{\partial x} + \nu\left(1+\frac{1}{\beta}\right)\frac{\partial^2 u}{\partial y^2} + \left(\frac{\sigma B^2(x)}{\rho} + \frac{\nu\phi}{k_1}\right)(u_e - u) \pm g\beta_T(T - T_\infty)\sin\frac{\Omega}{2} \tag{2}$$

$$u\frac{\partial T}{\partial x} + v\frac{\partial T}{\partial y} = \frac{k}{\rho c_p}\frac{\partial^2 T}{\partial y^2} + \frac{1}{\rho c_p}\left(1+\frac{1}{\beta}\right)\left(\frac{\partial u}{\partial y}\right)^2 + \frac{Q(x)}{\rho c_p}(T - T_\infty) \tag{3}$$

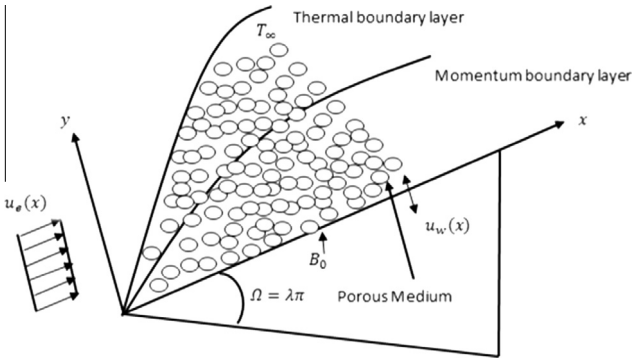

Figure 1 Physical model and coordinate system.

where u and v denote the velocity components in $x-$ and y-directions respectively, ν is kinematic viscosity, β is the Casson parameter, σ is the electrically conductivity, $B(x) = B_0 x^{(m-1)/2}$ [11] is magnetic field with B_0 the strength of the magnetic field, ρ is the fluid density, ϕ is the porosity, k_1 is the permeability of porous medium, g is the gravitational force due to acceleration, '+' sign corresponds to assisting flow, '−' is for opposing flow, β_T is the volumetric coefficient of thermal expansion, T is the fluid temperature, k is the thermal conductivity of the fluid, c_p is the specific heat at constant pressure and $Q(x) = Q_0 x^{m-1}$ is heat generation/absorption coefficient.

The corresponding boundary conditions are written as follows:

$$u = u_w(x),\ v = 0,\ T_w(x) = T_\infty + Ax^{2m} \text{ at } y = 0 \tag{4}$$

$$u \to u_e(x),\ T \to T_\infty \text{ as } y \to \infty, \tag{5}$$

Introduce the following similarity variables:

$$\psi = \sqrt{\frac{2\nu x u_e}{m+1}} f(\eta),\ \eta = \sqrt{\frac{(m+1)u_e}{2x\nu}} y,\ \theta = \frac{T - T_\infty}{T_w - T_\infty} \tag{6}$$

where the stream function ψ is defined by the following relations:

$$u = \frac{\partial \psi}{\partial y}, v = -\frac{\partial \psi}{\partial x}$$

From Eq. (6) in above equation, we can write

$$u = u_e(x) f'(\eta),\ v = \sqrt{\frac{\nu(m+1)u_e}{2x}} \left[f + \left(\frac{m-1}{m+1} \right) \eta f'(\eta) \right] \tag{7}$$

From Eqs. (2)–(7), one arrives at the following non-dimensional system:

$$\left(1 + \frac{1}{\beta}\right) f''' + ff'' + \lambda(1 - f'^2) + (M^2 + K)(1 - f') + \lambda_T \theta \sin\frac{\Omega}{2} = 0 \tag{8}$$

$$\theta'' + Pr f\theta' - 2\lambda Pr f'\theta + Pr\left(1 + \frac{1}{\beta}\right) Ec(f'')^2 + (2 - \lambda) Pr\varepsilon\theta = 0 \tag{9}$$

$$f'(\eta) = \gamma,\ \theta'(\eta) = 1 \text{ at } \eta = 0 \tag{10}$$

$$f'(\eta) = 1,\ \theta(\eta) = 0 \text{ as } \eta \to \infty \tag{11}$$

Here magnetic parameter, $M^2 = \frac{2\sigma B_0^2}{\rho U_\infty (m+1)}$, Porosity parameter, $K = \frac{2\nu\phi x}{k_1(m+1)u_e}$, Reynold's number, $Re_x = \frac{x u_e}{\nu}$, Grashof number, $Gr_x = \frac{2g\beta_T T_\infty x^3}{\nu^2(m+1)}$, thermal buoyancy parameter, $\lambda_T = \pm \frac{Gr_x}{Re_x^2}$ ($\lambda_T > 0$ corresponds to assisting flow and $\lambda_T < 0$ is for opposing flow), Prandtl number, $Pr = \frac{\mu c_p}{\alpha}$, Eckert number, $Ec = \frac{u_e^2(x)}{c_p(T_w - T_\infty)}$, heat generation/absorption parameter, $\varepsilon = \frac{Q_0}{c_p U_\infty}$ and Moving wedge parameter, $\gamma = \frac{U_w}{U_\infty}$.

The skin friction coefficient Cf_x and local Nusselt number Nu_x are defined as

$$Cf_x = \frac{\tau_w}{\rho u_e^2},\ Nu_x = \frac{x q_w}{k(T_w - T_\infty)} \tag{12}$$

where τ_w and q_w are the wall skin friction and wall heat flux, respectively, defined by

$$\tau_w = \mu_B \left(1 + \frac{1}{\beta}\right) \left[\frac{\partial u}{\partial y}\right]_{y=0},\ q_w = -\left(\frac{\partial T}{\partial y}\right)_{y=0} \tag{13}$$

Using Eqs. (6) and (13), Eq. (12) will take the form of

$$(Re_x)^{1/2} Cf_x \sqrt{\frac{2}{m+1}} = \left(1 + \frac{1}{\beta}\right) f''(0),$$
$$(Re_x)^{-1/2} Nu_x \sqrt{\frac{2}{m+1}} = -\theta'(0), \tag{14}$$

The system of Eqs. (8) and (9) along with the corresponding boundary conditions (10) and (11) are solved numerically by using finite difference scheme known as Keller-box method [25]. Results are computed and presented in tables graphically.

3. Results and discussion

In this section, the numerical results for velocity ($f'(\eta)$) and temperature ($\theta(\eta)$) with corresponding boundary conditions as well as skin friction coefficient $\left(\left(1 + \frac{1}{\beta}\right) f''(\eta)\right)$ and Nusselt number ($-\theta'(\eta)$) have been computed and presented graphically in Figs. 2–21. These results demonstrate the effects of Casson fluid parameter β, Pressure gradient parameter λ, magnetic parameter M, porosity parameter K, thermal buoyancy parameter λ_T, Prandtl number Pr, Eckert number Ec, heat generation/absorption parameter ε and moving wedge parameter γ. In order to check the validity of present method, the results are compared with results of existing literature, and shown in Tables 1–3.

Tables 1 and 2 illustrate the comparison of local skin friction coefficient for different values of m with the results of Watanabe [4], Kumari et al. [6], Ganapathirao et al. [23], Ishak et al. [8], Yih [16], Cebeci and Bradshaw [25] and Mukhopadhyay et al. [12], and are found in excellent agreement. It is also observed from these tables that local skin friction coefficient increases with the increase of m. Table 3 demonstrates the comparison of rate of heat transfer coefficient for different values of Pr. The comparison is made with the results of Lin and Lin [3], Yih [16] and Chamkha et al. [7] and revealed good agreement. It is also found that rate of heat transfer coefficient is higher for large values of Pr.

Table 4 describes the variation of wall shear stress and heat transfer rate obtained from the present method for increasing values of pertinent parameters.

Figs. 2–9 demonstrate the variation of velocity profile for various values of β, λ, M, K, λ_T, γ, Ec and ε, respectively. Fig. 2 shows the effect of β on velocity profile for various values of λ_T. It is worth mentioning here that $\beta \to \infty$ corresponds to Newtonian fluid, ($\lambda_T > 0$) represents assisting flow, ($\lambda_T < 0$) denotes opposing flow and ($\lambda_T = 0$) is for force convection flow. It is found that velocity is an increasing function of β in all cases of λ_T. The reason behind this is that increase of β leads to decrease in yield stress p_y, and consequently, reduces momentum boundary layer thickness. It is also observed that velocity is higher in case of Newtonian fluid for assisting flow ($\lambda_T > 0$). Fig. 3 illustrates the effect of λ on velocity profile for Newtonian and Non-Newtonian fluids. It is noteworthy that $\lambda > 0$ corresponds to decreasing pressure, $\lambda = 0$ represents flat plate case and $\lambda < 0$ shows increasing pressure case. It is observed that fluid velocity increases when $\lambda < 0$, and reduces when $\lambda > 0$. Interestingly, velocity is higher for Newtonian

Table 1 Comparison of coefficient of local skin friction $f''(0)$ for different values of m with $Pr = 0.73$, $M = K = \lambda_T = Ec = \varepsilon = \gamma = 0$ and $\beta \to \infty$. Where $\lambda = 2m/m + 1$.

$f''(0)$					
m	Watanabe [4]	Kumari et al. [6]	Ganapathirao et al. [23]	Ishak et al. [8]	Present results
0	0.46960	0.46975	0.46972	0.4696	0.4696
0.0141	–	0.50472	0.50481	0.5046	0.5046
0.0435	0.56898	0.56904	0.56890	0.5690	0.5690
0.0909	0.65498	0.65501	0.65493	0.6550	0.6550
0.1429	0.73200	0.73202	0.73196	0.7320	0.7320
0.2000	0.80213	0.80214	0.80215	0.8021	0.8021
0.3333	0.92765	0.92766	0.92767	0.9277	0.9277
0.5000	1.03890	–	1.03890	–	–
1	–	–	–	1.2326	1.2326
5	–	–	–	1.5504	1.5504
100	–	–	–	1.6794	1.6794
∞	–	–	–	1.6872	1.6872

Table 2 Comparison of skin friction coefficient $f''(0)$ for various values of m for Newtonian Fluid, where $\lambda = 2m/m + 1$.

$f''(0)$				
m	Yih [16]	Cebeci and Bradshaw [25]	Mukhopadhyay et al. [12]	Present results
−0.05	0.213484	0.21351	0.213802	0.21321
0.0	0.332057	0.33206	0.332206	0.33206
0.3333	0.757448	0.75745	0.757586	0.75743
1	1.232588	1.23259	1.232710	1.23259

Table 3 Comparison of coefficient of local skin friction $-\theta'(0)$ for different values of Pr with $\lambda = M = K = \lambda_T = Ec = \varepsilon = \gamma = 0$ and $\beta \to \infty$.

$-\theta'(0)$				
Pr	Lin and Lin [3]	Yih [16]	Chamkha et al. [7]	Present results
1	0.332057	0.332057	0.332173	0.3320
10	0.728148	0.728141	0.72831	0.7281
100	1.57186	1.571831	1.57218	1.5718
1000	3.38710	3.387083	3.38809	3.3881
10,000	7.29742	7.297402	7.30080	7.3102

fluid as compared to Non-Newtonian fluid. Furthermore, thickness of momentum boundary layer increases as λ increases. To illustrate the effect of M on velocity profile both assisting and opposing flows are presented in Fig. 4. It is observed that increasing values of M leads to increase the fluid flow in both cases of assisting and opposing flows. Physically, M is the ratio of electromagnetic force to viscous force, therefore increasing values of M means decreasing the viscous force that results in reduction in velocity boundary layer thickness.

Fig. 5 reveals the effect of K on velocity profile for various values of λ. It needs to mention that $K = 0$ represents non-porous medium, whereas $K \neq 0$ is for porous medium. It is noticed that velocity of fluid is higher for higher values of K. Porosity is defined as the measure of void (or empty) spaces in a porous medium and is a fraction of the volume of voids over the total volume. Convection flows are often influenced by porosity and in result raise the fluid velocity. The effect of λ_T on velocity profile for various γ is exhibited in Fig. 6. The velocity is found increasing for assisting flow ($\lambda_T > 0$) while decreases for opposing flow ($\lambda_T < 0$). This phenomenon can be supported by the fact that buoyancy force is stronger for assisting flow and weaker for the opposing flow. It is also found that momentum boundary layer thickness decreases rapidly for assisting flow as wedge is moving in flow direction. Fig. 7 elucidates the effect of γ on velocity profile in porous and non-porous medium. It is worth to mention that $\gamma < 0$ corresponds to the case when wedge is moving opposite to the fluid motion, $\gamma = 0$ represents static or stationary wedge case and $\gamma > 0$ is the case when wedge and fluid move in the same direction. It is noticed that velocity is increasing function of γ. It is also noticed that velocity of fluid merely squeezes closer and closer to the wall when wedge and fluid move in one direction through porous medium.

The influence of Ec on velocity profile for assisting and opposing flows is shown in Fig. 8. It is interesting to note that for assisting flow, fluid velocity rises for increasing values of Ec while for opposing flow, it falls as Ec increases. It is noteworthy here that increasing values of Ec have no effect on velocity profile when $\lambda_T = 0$. Fig. 9 exhibits the effect of ε on velocity profile in porous and non-porous medium. It is important to note that $\varepsilon > 0$ is for heat generation and $\varepsilon < 0$ corresponds to heat absorption case. It is found that velocity is higher for increasing values of ε. It is also seen that momentum boundary layer becomes thinner as ε increases in presence of porous medium.

In Figs. 10–18, numerical results are displayed graphically for dimensionless temperature profile for different values of β, λ, M, K, λ_T, γ, Ec, ε and Pr, respectively. Fig. 10 shows the effect of β on dimensionless temperature profile for various values of λ_T. A decrease in fluid temperature is seen for increasing values of β in all cases of λ_T. A decrease in thermal boundary layer thickness is also observed. Fig. 11 is depicted to get insight of the effect of λ on dimensionless temperature profile in porous and non-porous medium. It is interesting to see that in both cases of porous and non-porous medium, fluid temperature decreases when $\lambda > 0$ and increases when $\lambda < 0$. It is also

Table 4 Numerical results for skin friction coefficient and Nusselt number for different values of β, λ, M, K, λ_T, Pr, γ, E_c and ε.

β	λ	M	K	λ_T	Pr	γ	Ec	ε	$(1+1/\beta)f''(0)$	$-\theta'(0)$
0.6	0.4	0.2	0.6	0.3	0.72	0.3	0.4	0.2	1.5274	0.4650
0.8									1.4064	0.4835
2									1.1552	0.5262
	0.6								1.6489	0.5861
	1.5								2.1192	0.9761
		0.8							1.7683	0.4601
		1.2							2.0455	0.4515
			0.8						1.6118	0.4636
			1.5						1.8771	0.4570
				0					1.4240	0.4659
				−0.2					1.3542	0.4660
					1				1.5206	0.5052
					3				1.5010	0.6115
						0			2.0278	0.1939
						−0.3			2.4473	−0.1312
							0.8		1.5323	0.3403
							1.2		1.5373	0.2144
								0.5	1.5433	0.1781
								0.8	1.5755	−0.1265

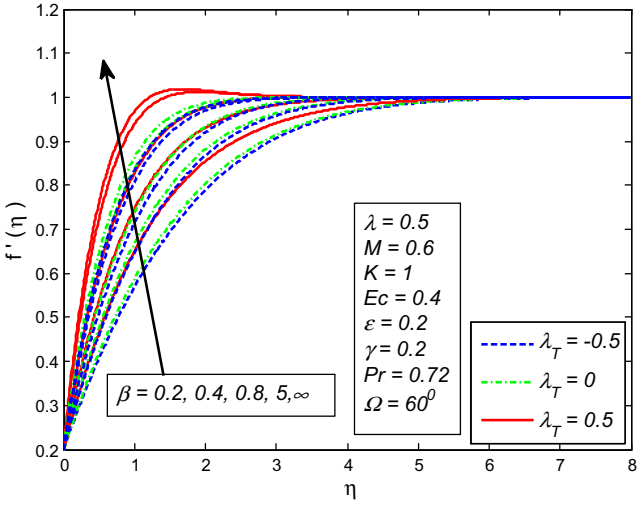

Figure 2 Effect of β on velocity for various λ_T.

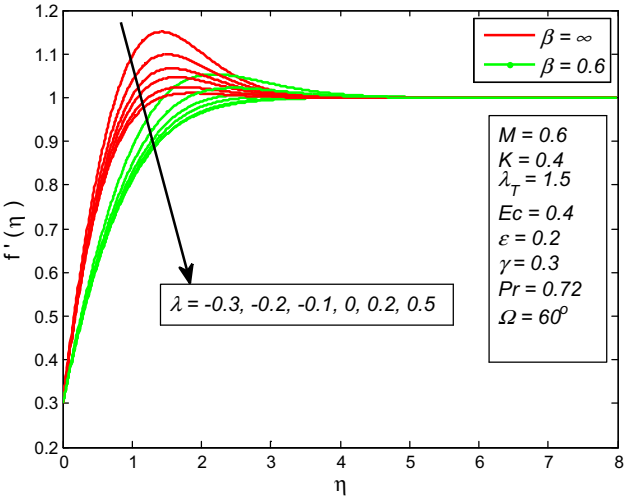

Figure 3 Effect of λ on velocity for different β.

noticed that in case of decelerated flow temperature gets peak values near the wall and then gradually decreases as moving away. To demonstrate the effect of M on temperature profile both assisting and opposing flows are depicted in Fig. 12. It is found that fluid temperature is lower for increasing values of M. It is well known fact that Lorentz force generates in electrically conducting fluid, which reduces thickness of thermal boundary layer and consequently temperature falls.

Fig. 13 exhibits the influence of K on dimensionless temperature profile for different values of γ. It is noticed that in all cases of γ, temperature falls as K increases. It is also seen that temperature increases near the wall when wedge and fluid have opposite direction. Further, temperature reduces slightly when $\gamma < 0$. A similar behavior is observed for increasing value of λ_T on temperature for $\lambda < 0$ and $\lambda > 0$ (see Fig. 14). The reason behind this is that, λ_T is defined as the ratio of buoyancy force to viscous force in the boundary region; therefore, buoyancy force implies a rise in rate of heat transfer resulting in decrease in temperature. To get insight of the variation of dimensionless profile for increasing values of γ, Fig. 15 is plotted. It is found that temperature is decreasing function of γ. Temperature peak values are also observed near the boundary in the presence of viscous dissipative heat when $\gamma < 0$. Furthermore, rapid decrease in thermal boundary layer thickness is also seen when $\gamma > 0$.

Fig. 16 displays the effect of Ec on temperature profile for different values of γ. It is seen that temperature is higher for larger values of Ec. The explanation for this phenomenon is that in moving fluid heat energy is stored because of frictional heating, and results in higher temperature. In addition to this, stronger viscous dissipative heat causes an increase in fluid temperature. It is also very interesting to note that temperature overshoots near the wall as Ec increases when wedge is moving opposite in fluid direction ($\gamma < 0$). The effect of ε on dimen-

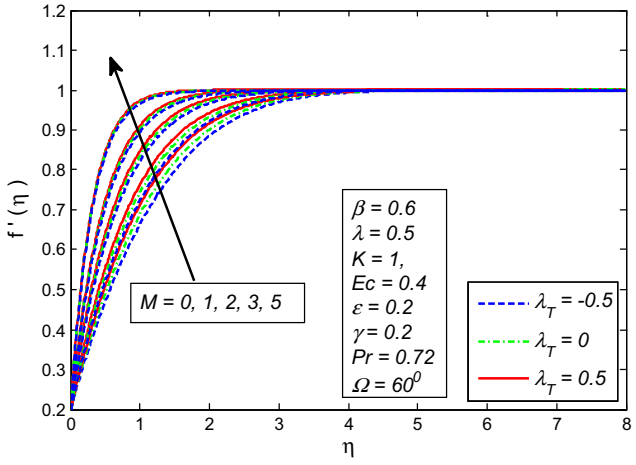

Figure 4 Effect of M on velocity for various λ_T.

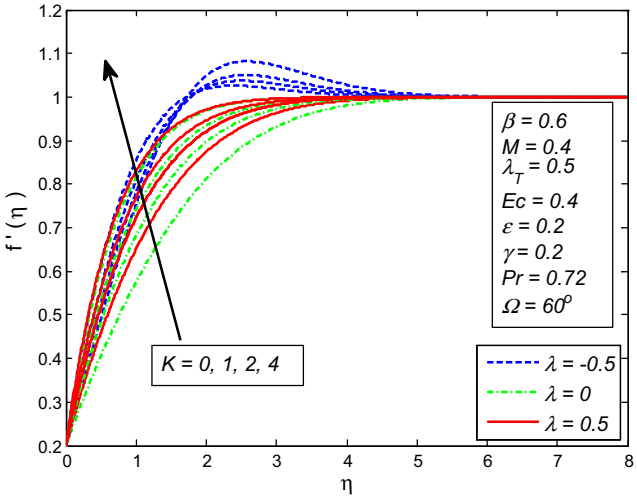

Figure 5 Effect of K on velocity for various λ.

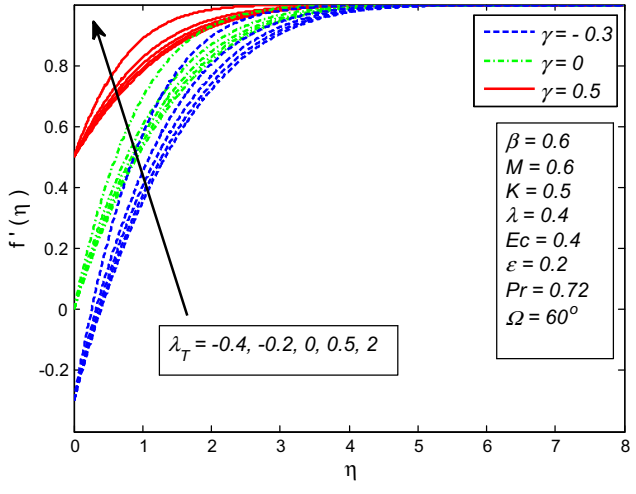

Figure 6 Effect of λ_T on velocity for various γ.

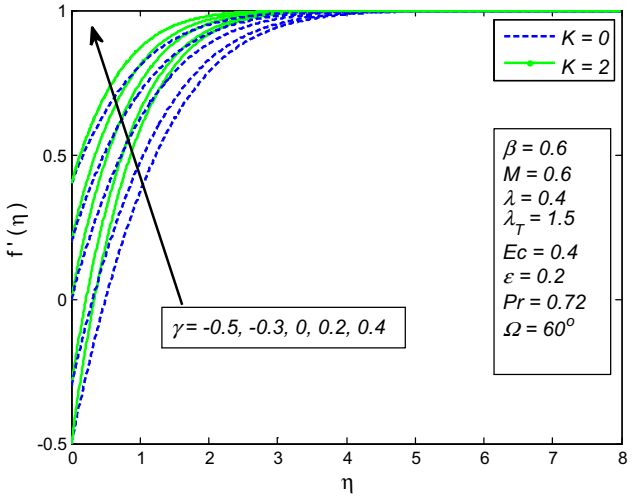

Figure 7 Effect of γ on velocity for various K.

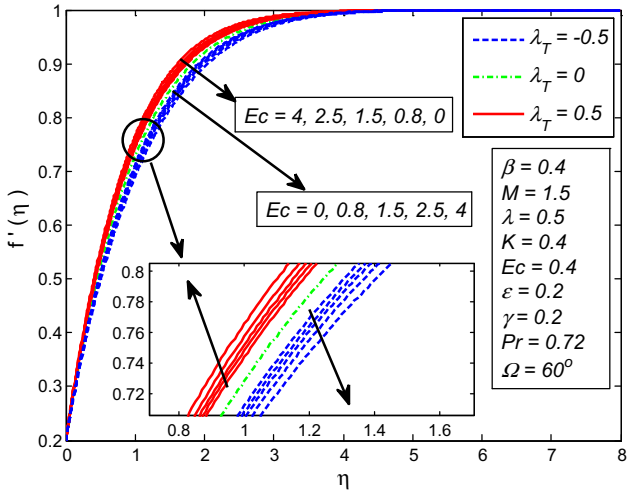

Figure 8 Effect of Ec on velocity for various λ_T.

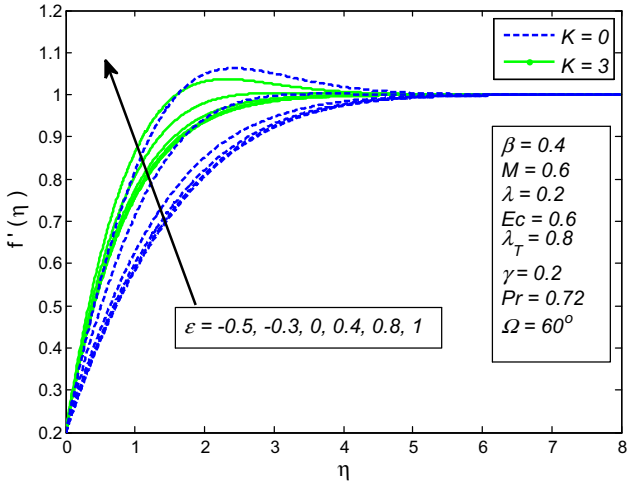

Figure 9 Effect of ε on velocity for two different values of K.

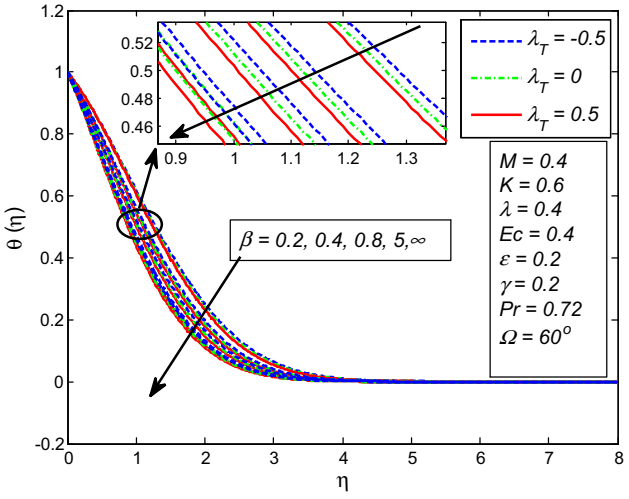

Figure 10 Effect of β on temperature for various λ_T.

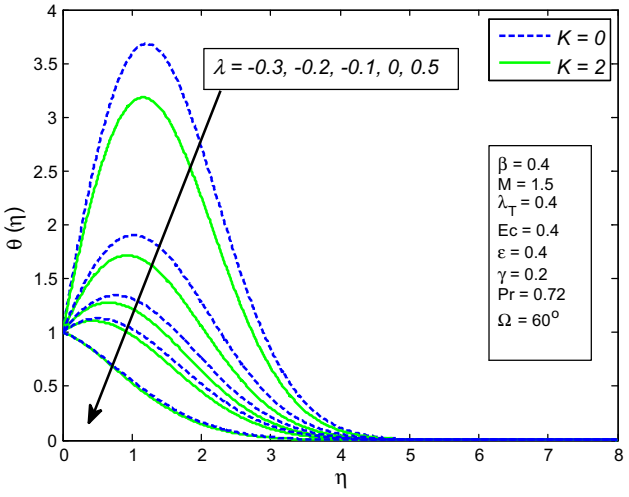

Figure 11 Effect of λ on temperature for various S.

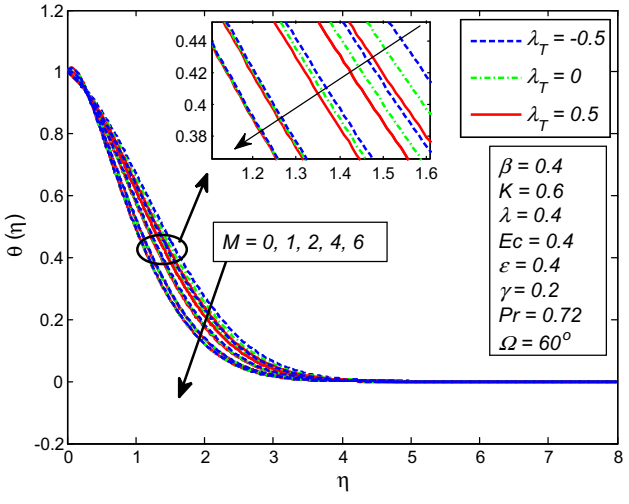

Figure 12 Effect of M on temperature for various λ_T.

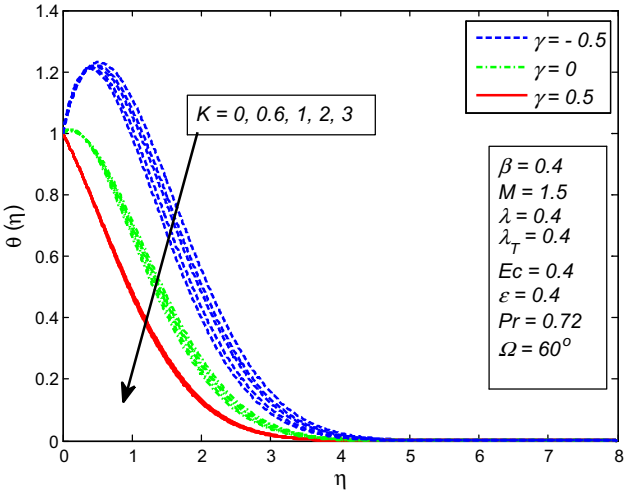

Figure 13 Effect of K on temperature for various γ.

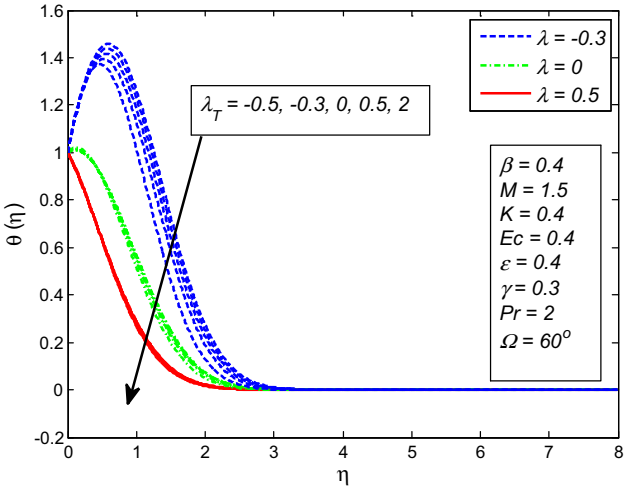

Figure 14 Effect of λ_T on temperature for various λ.

sionless temperature profile for various values of γ is provided in Fig. 17. It is noticed that temperature enhances for $\varepsilon > 0$. Physically, increasing heat source implies more energy produces resulting in temperature enhancement. On the other hand when $\varepsilon < 0$ it has opposite behavior. In simple word, heat generation has tendency to enhance the fluid temperature, while heat absorption decreases it. Also, for $\varepsilon > 0$ temperature peak occurs near wall of the wedge. Nevertheless, it is evident that temperature decreases significantly, when wedge and fluid move in same direction.

The influence of Pr on dimensionless temperature profile for assisting and opposing flows is displayed in Fig. 18. Interestingly, fluid temperature increases close to wall and then merely reduces for increasing values of Pr. As expected, rate of thermal diffusion is lowered as Pr increases. In short, higher values of Pr lead to decrease in thermal boundary layer thickness. Consequently, temperature falls.

To illustrate the characteristics of local skin friction coefficient $\left(\left(1+\frac{1}{\beta}\right)f''(0)\right)$ and Nusselt number $(-\theta'(0))$ for different values of β, K, λ_T, γ, Ec, ε and Pr, Figs. 19–21 are

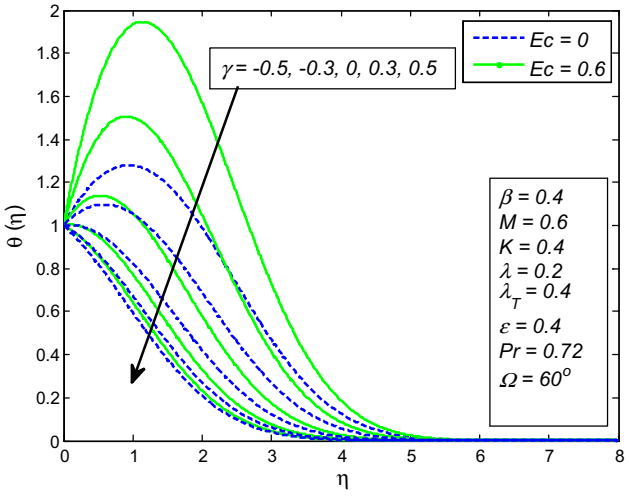

Figure 15 Effect of γ on temperature for different Ec.

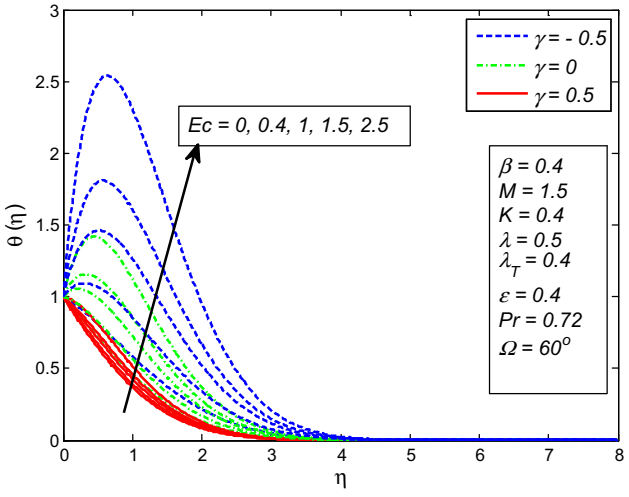

Figure 16 Effect of Ec on temperature for various γ.

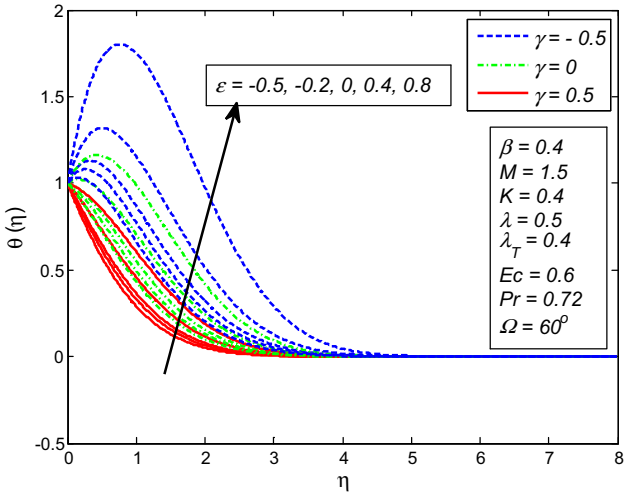

Figure 17 Effect of ε on temperature for various γ.

plotted, respectively. Fig. 19 displays the effect of local skin friction coefficient for different values of β, λ_T and γ. It is found that increasing values of λ_T enhance wall shear stress while it decreases with increase of β and γ. The variations of heat transfer coefficient for various values of Pr, Ec and ε are shown in Fig. 20. It is interesting to note that rate of heat transfer increases at the moving wedge surface as Pr increases when $Ec = 0$, whereas it starts decreasing for increasing values of Pr in presence of viscous dissipative heat ($Ec \neq 0$). This mechanism clearly shows that when heat is dissipated to the fluid through walls, it increases the thermal conductivity (or lower viscosity) of fluid, which results in a rise in boundary layer thickness and therefore, rate of heat transfer decreases at the wedge surface. Moreover, it is observed that rate of heat transfer is decreasing function of Ec and ε.

Finally, Fig. 21 reveals the variations of Nusselt number for different values of β, K and γ. It is noticed that rate of heat transfer is higher for increasing values of β and γ while rate of heat transfer falls as K increases.

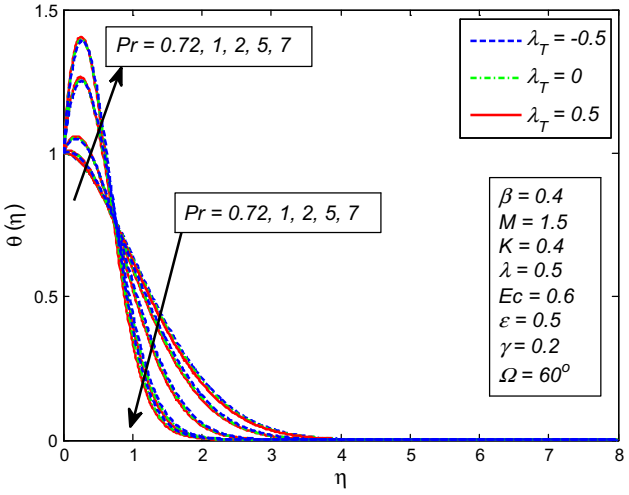

Figure 18 Effect of Pr on temperature for various λ_T.

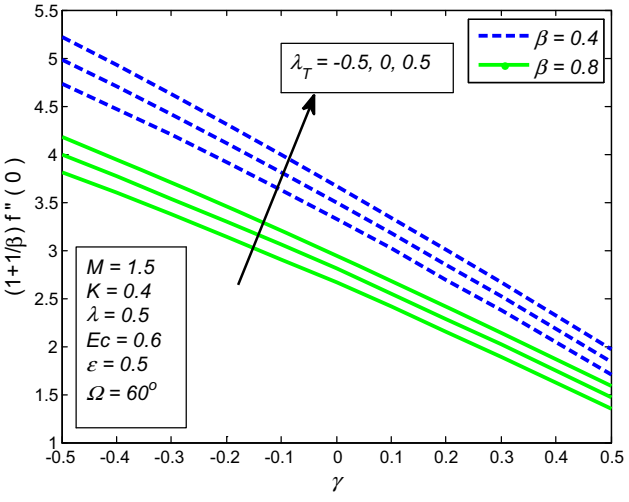

Figure 19 Variation of local skin friction for various β, γ and λ_T.

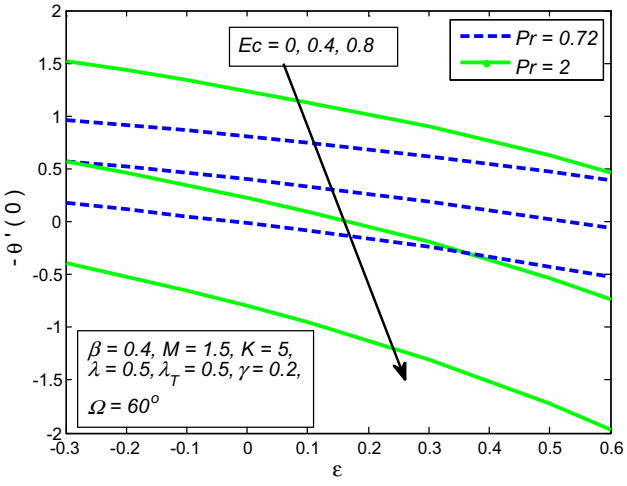

Figure 20 Variation of reduced Nusselt number for various Ec, ε and Pr.

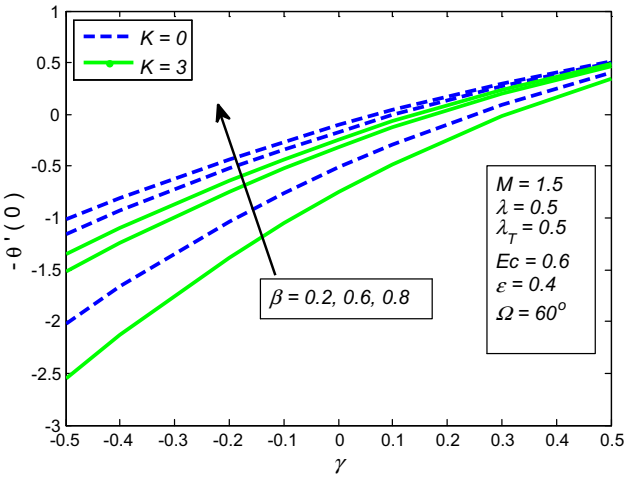

Figure 21 Variation of reduced Nusselt number for various K, γ and β.

4. Conclusions

This study reveals numerical investigation of mixed convection electrically conducting flow of Casson fluid along a moving wedge saturated in porous medium in presence of viscous dissipation and heat generation/absorption. The governing non-linear partial differential equations are transformed to nonlinear ordinary differential equations by using the similarity transformation, and then solved numerically by Keller-box method. The obtained results for local skin friction coefficient and heat transfer coefficient are compared with the results of existing literature. Effects of Casson parameter β, pressure gradient parameter λ, magnetic parameter M, porosity parameter K, thermal buoyancy parameter λ_T, moving wedge parameter γ, Eckert number Ec, heat generation/absorption parameter ε and Prandtl number Pr on velocity profile, temperature profile, wall shear stress and heat transfer rate are computed, displayed graphically and discussed. Some interesting findings are as follows:

- Fluid flow increases with the increase of β, M, K, λ_T and ε.
- Fluid velocity decreases with increase of λ.
- Fluid velocity increases with increase of Ec when $\lambda_T > 0$, and decreases when $\lambda_T < 0$.
- The dimensionless temperature decreases with the increase of β, λ, M, K, λ_T, γ and Pr.
- The dimensionless temperature increases with the increase of Ec and ε.
- The local skin friction coefficient increases with the increase of λ_T.
- The local skin friction coefficient decreases with the increase of β and γ.
- The rate of heat transfer increases with the increase of β and γ.
- The heat transfer rate decreases with increase of Ec, ε and K.
- The rate of heat transfer decreases with increase of Pr when $Ec \neq 0$ and increases when $Ec = 0$.

Acknowledgments

The authors would like to acknowledge Ministry of Higher Education (MOHE) and Research Management Centre Universiti Teknologi Malaysia (UTM) for the financial support through vote numbers 4F713, 4F538 and 06H67 for this research.

References

[1] V.M. Falkner, S.W. Skan, Some approximate solutions of the boundary-layer for flow past a stretching boundary, SIAM J. Appl. Math. 49 (1931) 1350–1358.

[2] K.R. Rajagopal, A.S. Gupta, T.Y. Na, A note on the Falkner-Skan flows of a non-Newtonian fluid, Int. J. Non Linear Mech. 18 (4) (1983) 313–320.

[3] H.T. Lin, L.K. Lin, Similarity solutions for laminar forced convection heat transfer from wedges to fluids of any Prandtl number, Int. J. Heat Mass Transfer 30 (6) (1987) 1111–1118.

[4] T. Watanabe, Thermal boundary layer over wedge with uniform suction or injection in force flow, Acta Mech. 83 (1990) 119–126.

[5] T. Watanabe, I. Pop, Magnetohydrodynamic free convection flow over a wedge in the presence of a transverse magnetic field, Int. Commun. Heat Mass Transfer 20 (6) (1993) 871–881.

[6] M. Kumari, H.S. Takhar, G. Nath, Mixed convection flow over a vertical wedge embedded in a highly porous medium, Heat Mass Transfer 37 (2001) 139–146.

[7] A.J. Chamkha, M. Mujtaba, A. Quadri, C. Issa, Thermal radiation effects on MHD forced convection flow adjacent to a non-isothermal wedge in the presence of a heat source or sink, Heat Mass Transfer 39 (2003) 305–312.

[8] A. Ishak, R. Nazar, I. Pop, Falkner-Skan equation for flow past a moving wedge with suction or injection, J. Appl. Math. Comput. 25 (1) (2007) 67–83.

[9] A. Ishak, R. Nazar, I. Pop, Moving wedge and flat plate in a micropolar fluid, Int. J. Eng. Sci. 44 (18–19) (2006) 1225–1236.

[10] K.L. Hsiao, MHD mixed convection for viscoelastic fluid past a porous wedge, Int. J. Non Linear Mech. 46 (1) (2011) 1–8.

[11] X. Su, L. Zheng, X. Zhang, J. Zhang, MHD mixed convective heat transfer over a permeable stretching wedge with thermal radiation and ohmic heating, Chem. Eng. Sci. 78 (2012) 1–8.

[12] S. Mukhopadhyay, I.C. Mondal, A.J. Chamkha, Casson fluid flow and heat transfer past a symmetric wedge, Heat Transfer Res. 42 (8) (2013) 665–675.
[13] M.M. Rashidi, M. Ali, N. Freidoonimehr, B. Rostami, and M. A. Hossain, Mixed Convective Heat Transfer for MHD Viscoelastic Fluid Flow over a Porous Wedge with Thermal Radiation, Adv. Mech. Eng. http://dx.doi.org/10.1155/2014/735939.
[14] N.T. El-dabe, A.Y. Ghaly, R.R. Rizkallah, K.M. Ewis, Numerical solution of MHD boundary layer flow of non-newtonian Casson fluid on a moving wedge with heat and mass transfer and induced magnetic field, J. Appl. Math. Phys. 3 (2015) 649–663.
[15] B. Gebhart, Effects of viscous dissipation in natural convection, J. Fluid Mech. 14 (2) (1962) 225–232.
[16] K.A. Yih, MHD forced convection flow adjacent to a non-isothermal wedge, Int. Commun. Heat Mass Transfer 26 (6) (1999) 819–827.
[17] R. Kandasamy, I. Muhaimin, A.B. Khamis, Thermophoresis and variable viscosity effects on MHD mixed convective heat and mass transfer past a porous wedge in the presence of chemical reaction, Heat Mass Transfer 2009 (45) (2009) 703–712.
[18] D. Pal, H. Mondal, Influence of temperature-dependent viscosity and thermal radiation on MHD forced convection over a non-isothermal wedge, Appl. Math. Comput. 212 (1) (2009) 194–208.
[19] M. Ganapathirao, R. Ravindran, I. Pop, Non-uniform slot suction (injection) on an unsteady mixed convection flow over a wedge with chemical reaction and heat generation or absorption, Int. J. Heat Mass Transfer 67 (2013) 1054–1061.
[20] K.V. Prasad, P.S. Datti, K. Vajravelu, MHD mixed convection flow over a permeable non-isothermal wedge, J. King Saud Univ. – Sci. 25 (4) (2013) 313–324.
[21] R. Ahmad, W.A. Khan, Effect of viscous dissipation and internal heat generation/absorption on heat transfer flow over a moving wedge with convective boundary condition, Heat Transfer Res. 42 (7) (2013) 589–602.
[22] M.S. Khan, I. Karim, M.S. Islam, M. Wahiduzzaman, MHD boundary layer radiative, heat generating and chemical reacting flow past a wedge moving in a nanofluid, Nano Converg. 1 (2014) 20.
[23] M. Ganapathirao, R. Ravindran, E. Momoniat, Effects of chemical reaction, heat and mass transfer on an unsteady mixed convection boundary layer flow over a wedge with heat generation/absorption in the presence of suction or injection, Int. J. Heat Mass Transfer 51 (2015) 289–300.
[24] R.M. Kasmani, S. Sivasankaran, M. Bhuvaneswari, Z. Siri, Effect of chemical reaction on convective heat transfer of boundary layer flow in nanofluid over a wedge with heat generation/absorption and suction, J. Appl. Fluid Mech. 9 (1) (2016) 379–388.
[25] T. Cebeci, P. Bradshaw, Physical and Computational Aspects of Convective Heat Transfer, 1st ed., Springer Verlag, 1984.